Large scale volume holographic storage in the Long Interaction Length Architecture

Geoffrey W. Burr, Fai H. Mok,[1] and Demetri Psaltis

Electrical Engineering Department, MS 116–81
California Institute of Technology
Pasadena, CA 91125

ABSTRACT

We describe a page–formatted random–access holographic memory designed to store up to 160,000 holograms. The memory consists of 16 vertically spaced locations, each containing 10,000 holograms, which in turn are organized as 10 fractal–multiplexed rows of 1000 angularly–multiplexed holograms. A segmented mirror array is used to enable random access to any of the stored holograms within the access time of a non–mechanical angle scanner such as an acousto–optic deflector. Using a mechanical scanner with such a mirror array, we demonstrate storage of 10,000 holograms at a single location of the system, as well as simultaneous storage and recall of holograms at 6 locations, including the highest and lowest of the 16 locations.

INTRODUCTION

Volume holographic data storage involves the superposition and independent recall of multiple pages of data within the same volume of a storage medium. These pages, stored as separate holograms, are accessed by changing either the angle,[1] wavelength,[2,3] or phase code[4,5] of the reference beam used to store and retrieve them. The storage capacity C achievable with each of these methods can be written as

$$C = NM,$$

where N is the number of bits in each stored page, and M is the number of pages superimposed in the same volume. Assuming one bit per pixel, current spatial light modulator (SLM) technology can provide 10^5—10^6 bits per stored page. There are two limiting factors on the number of holograms that can be multiplexed in the same location. The first is the number of distinct reference angles (or wavelengths or phase codes) that can be generated. The second is the finite material dynamic range, which causes the diffraction efficiency of each hologram to decay as $1/M^2$.[6] In the next section, we describe an architecture we call the Long Interaction Length Architecture (LILA), which has allowed us to store M=10,000 holograms at a single location.

LONG INTERACTION LENGTH ARCHITECTURE

The Long Interaction Length Architecture is shown in Figure 1. The object beam enters the small end face of a long rectangular crystal bar and propagates the length of the crystal—the wide reference beam enters the orthogonal face and meets it at 90°. This configuration is convenient for several reasons. First, the Bragg selectivity is maximal for this geometry, allowing optimal use of the angular scanning range of the reference beams. Second, the interaction length can be increased simply by extending the length of the crystal, which increases diffraction efficiency as well as Bragg selectivity. Finally, the path over which fanning of the strong reference beam can occur is set by the width of the object beam, not by the interaction length. There are a few drawbacks, including the smaller electrooptic coefficient, the

[1]also affiliated with Holoplex, 600 South Lake Avenue, Suite 102, Pasadena, CA 91106

0-8194-1621-5/94/$6.00

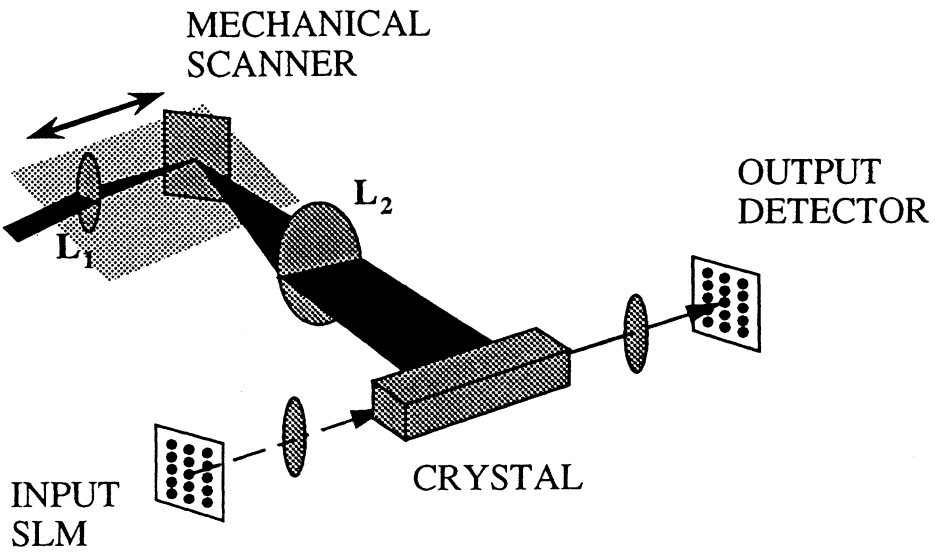

Figure 1: The Long Interaction Length Architecture.

increased $e^{-\alpha L}$ loss, and the decreased photorefractive response at the relatively high spatial frequencies being stored. In general, the LILA geometry augments the geometry limit on the number of distinct reference beams at the expense of the dynamic range limit.

Using the system shown in Figure 1, we stored 10,000 image plane holograms in an 8×8×50 mm bar of 0.01% Fe–doped $LiNbO_3$.[7] The **c**–axis was at 45% to the vertical faces. The reference beam was 45mm × 5mm in area, and the object beam 4mm × 5.4mm for a total interaction volume of 0.972 cm^3. The SLM was demagnified by a factor of 5 and imaged to a plane located approximately halfway along the long dimension of the crystal. Each hologram contained 480 × 440 pixels, so that assuming one bit per pixel, 2.11 GBits were stored. Using a final exposure of 0.21 seconds and an erasure time constant of 2250 seconds, a standard recording schedule was computed.[6] This led to a initial exposure of 3.1 seconds and a total exposure time of 102 minutes. The average exposure time was 0.61 seconds. The actual time required to complete recording was significantly longer since we included extra delays between each exposure for the mechanical scanner and video input to stabilize.

A 4–F system was used to magnify and image the reference beams onto the long face of the crystal, with a mirror at 45° near the center focal plane to fold the optical axis by 90° (See Figure 1). Lens L_1 and the mirror were fixed relative to each other and mounted on a linear actuator capable of 4 inches of travel parallel to the incoming reference beam, while lens L_2 and the crystal were mounted on the optical table. By moving the linear actuator back and forth, the focused spot at the folding mirror was translated horizontally in the back focal plane of lens L_2. This translation appeared at the crystal as changes in the horizontal incidence angle of the reference beam, enabling angular multiplexing.

The experimentally measured selectivity of 1.1×10^{-5} radians (all angles external to the crystal) agreed with theoretical expectations for the 90° geometry and a 45mm interaction length. Although the presence of images broadened the effective selectivity by a factor of 2 or so, a spacing of 4×10^{-5} radians was sufficient to suppress holographic readout by 30dB. To implement this spacing with a lens L_2 of focal length 150mm, the linear actuator was moved 6μm between holograms for a total travel of 60mm.

The input images during the experiment included gray–scale cartoon images as well as a benchmark chessboard pattern. Several reconstructions of this chessboard pattern are shown in Figure 2. The hologram number appears in the upper left corner of each hologram. As can be seen, the time constant used was too high, and the early holograms decayed more than expected. The average diffraction efficiency of the chessboard images was measured to be about 5×10^{-9}, so the power in the reconstructed holograms

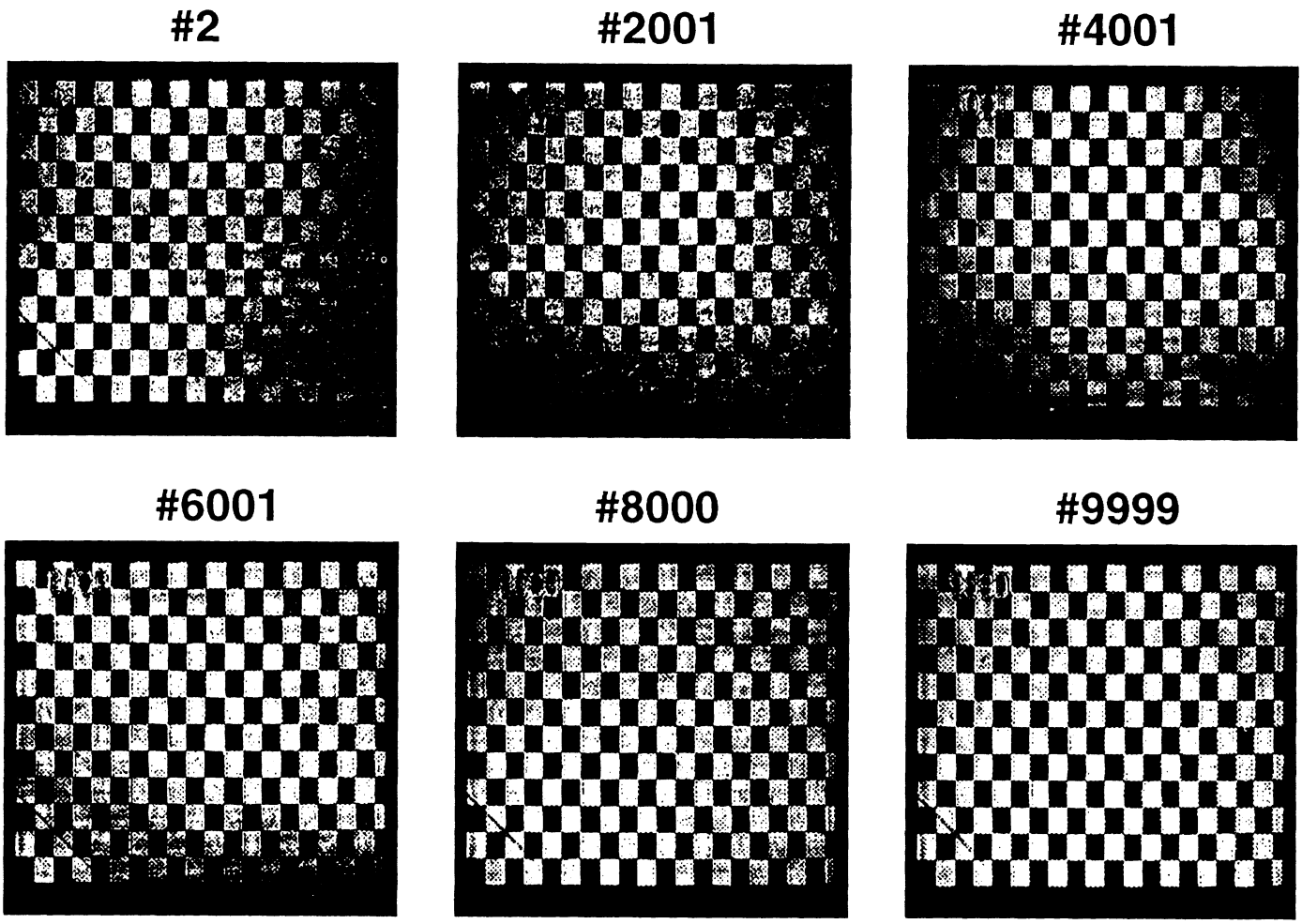

Figure 2: Reconstructions from storage of 10,000 image plane holograms.

was within the same order of magnitude as the background light scattered by the crystal. Fanning of the reference beam did not appear to affect storage.

At this point, we can store 10,000 holograms at each location. Incorporating the SLM limits mentioned in the introduction, the total achievable storage capacity at one location is therefore between 1 and 10 gigabits. In order to increase the capacity beyond this limit, we can use spatial multiplexing—in which angle, wavelength, or phase code multiplexed holograms are stored at multiple locations.

SPATIAL MULTIPLEXING AND RANDOM ACCESS

Spatial multiplexing has been used for holographic storage in both 2–D and 3–D media.[8–14] Two general methods have been under general consideration for accomplishing simultaneous spatial and angular multiplexing in 3–D media. The first involves mechanically moving the storage medium to access different spatial locations.[12,13] The second method uses acoustooptic deflectors (AODs) to perform both angle and spatial multiplexing,[8–11,14] which leads to fast access at the expense of a more complex optical system. In addition, since the AOD delay is essentially the time needed to fill the optical aperture with the next acoustic grating, the access time is independent of the order in which the holograms are accessed, providing random access.

The first to demonstrate non–mechanical spatial multiplexing was Huignard *et al* in the early 1970's[9,10].

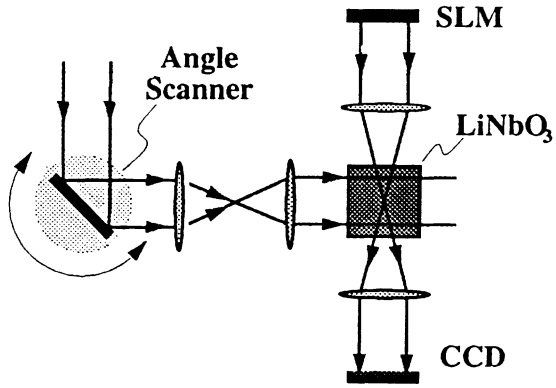

Figure 3: Angle–multiplexed holographic memory using an angle scanner.

Their system used two cascaded AOD deflectors to supply the same 2–D spatial translation to both the reference and object arms. A reflection grating combined the beams at the crystal surface. Angle multiplexing at each location was performed by a mechanically rotating beam shearing element placed in the reference arm. Using this arrangement, they were able to store 10 holograms at each of 25 locations.

The key element in our realization of angle and spatial multiplexing is a segmented mirror array, which preserves horizontal angular multiplexing while using vertical deflection to step between distinct storage locations. In the next section, we describe the operation of such a mirror array. We also briefly outline our initial Holographic Random Access Memory (HRAM) design.[11,14]

SEGMENTED MIRROR ARRAY

The motivation behind the mirror array is similar to that used in the deflection system in the LILA experiment described above. Consider a standard angle–multiplexing setup, as shown in Figure 3. The deflection created by the angle scanner in the reference arm is imaged to the surface of the crystal with a 4–F system. If a fixed mirror is placed in the center focal plane at 45° to the optical axis, the 4–F system contains a right–angle turn, but is otherwise identical in operation (See Figure 4b). Operation of the angle deflector causes the focused spot to trace a horizontal path across the surface of the fixed mirror. If we were to remove all of the mirror surface above and below this horizontal path, leaving only a thin mirror strip, the operation of the system would be unchanged. We can then place additional mirror strips in this newly vacated region, and orient each with its own fixed deflection angle, creating a vertically stacked array of mirror strips,

Figures 4a and 4b diagram the operation of such a mirror array—Figure 4a shows selection of output location by the vertical angle scanner (AOD), while Figure 4b shows angle multiplexing at a spot by the horizontal AOD. The deflection angle of the vertical AOD determines which mirror strip will be illuminated. Each mirror strip is tilted in both dimensions in order to redirect incident light to one of the 16×16 locations of the crystal. As a result, the illuminated mirror strip directs the incoming reference beam to the corresponding location on the crystal.

Since the mirror strips are stacked in the vertical direction but extend horizontally, the horizontal AOD moves the focused spot along the same mirror strip. This motion in the Fourier plane of the output lens results in a change of horizontal incidence angle at the crystal, without any motion of the spot itself. In summary, the horizontal AOD provides angle multiplexing at any given location, while the vertical AOD selects which location is to be illuminated.

The drawings show the mirror strips at 45° to the incoming beam because the operation of the mirror array is easier to explain this way. In the actual implementation (shown in Figure 10), a beamsplitter is required because the surface of the mirror array must be aligned with the focal plane (the center of

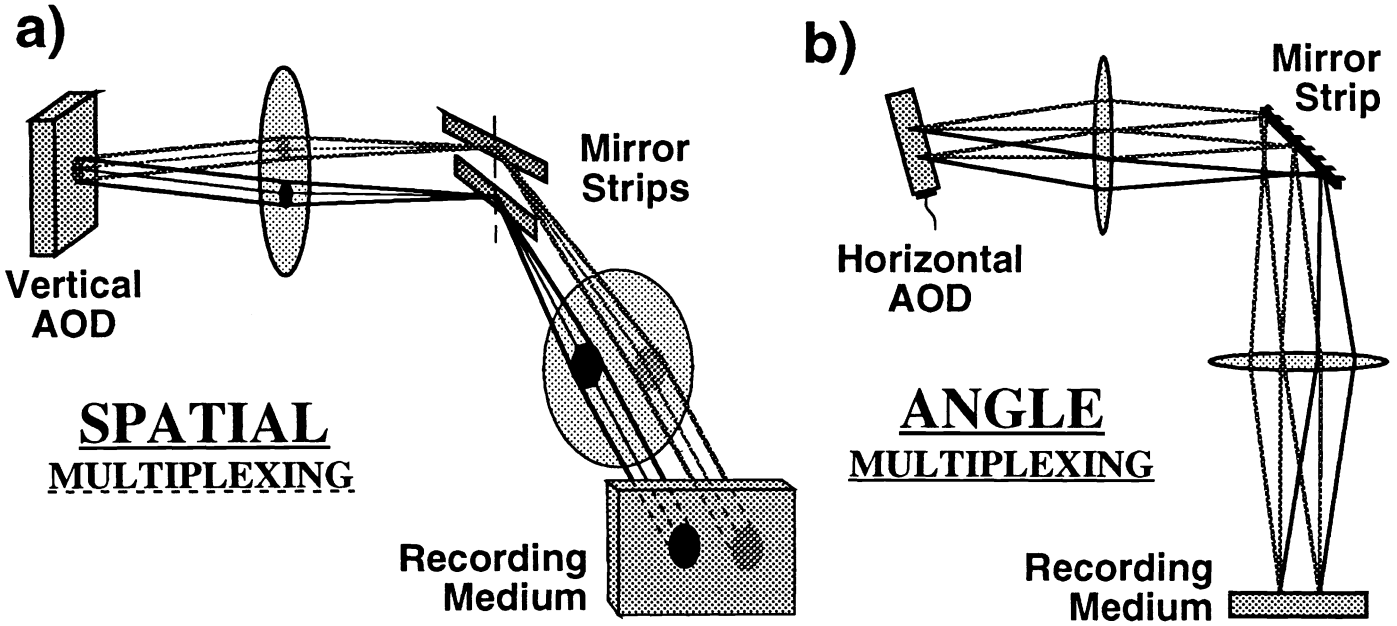

Figure 4: Operation of the mirror array. (a) Selection of output location by vertical angle scanner. (b) Angle multiplexing by horizontal angle scanner.

the 4–F system directing the reference beam to the crystal), in which the converging beams achieve their focus. This allows us to minimize the vertical size of each mirror strip that is necessary to avoid crosstalk to other storage locations.

The schematic of the mirror array is shown in Figure 5. There are 256 mirror strips—one for each location on the crystal. Each is 150μm wide and 75mm long. The mirror array is composed of 16 "tiles," each of which has 16 mirror strips cut as grooves. The change in angle between tiles and between groove faces is 0.5°. The angular change between tiles is orthogonal to the increment between grooves, allowing tilting of individual facets in both directions.

A prototype mirror array was constructed with blazed grating technology. This technique involves using a diamond tip to cut grooves on suitable substrates. The groove angles are accurately controlled by the tilt of the diamond tip with respect to the substrate. The width of each groove is set by the dimensions of the diamond itself. A photograph of the completed mirror array is shown in Figure 6.

The HRAM architecture for non–mechanical spatial and angle multiplexing is shown in Figure 7. The functionality of this architecture was described in detail in references [11,14]. The storage medium is a photorefractive crystal such as $LiNbO_3$. Holograms are stored at a 16 by 16 grid of locations on the crystal, with 4000 holograms per location. Note the presence of electro–optic modulators which compensate the Doppler shifts introduced by the operation of the AODs. The lenslet array magnifies the SBP delivered by the object arm AODs so that, in each dimension, 1000 resolvable spots can be delivered at each of the 16 locations.[11,14]

Since current AOD technology can provide SBP on the order of 1000 or so, storage of up to 10000 holograms at each location of the above system is problematic. The horizontal AOD is overloaded by the large number of angles required, while the vertical AOD is underutilized. One solution is to use multiple mirror facets for each location, reducing the number of angularly multiplexed holograms required per facet. This can be accomplished using fractal multiplexing.

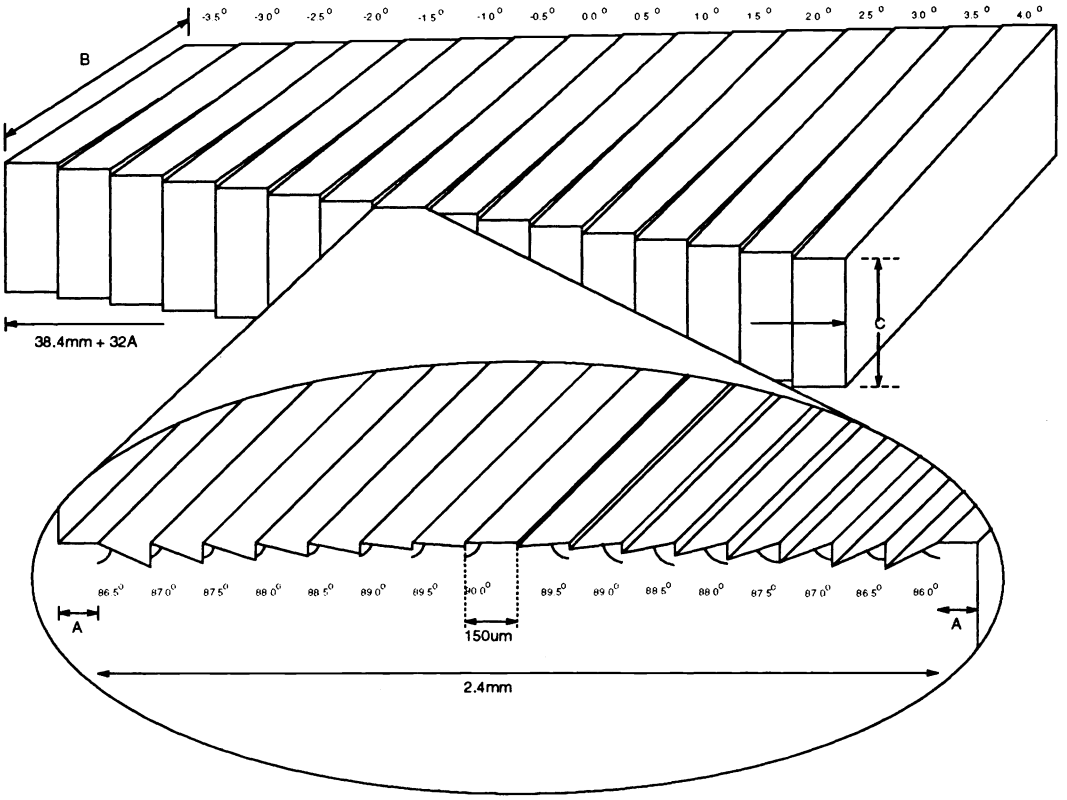

Figure 5: Mirror Array Schematic.

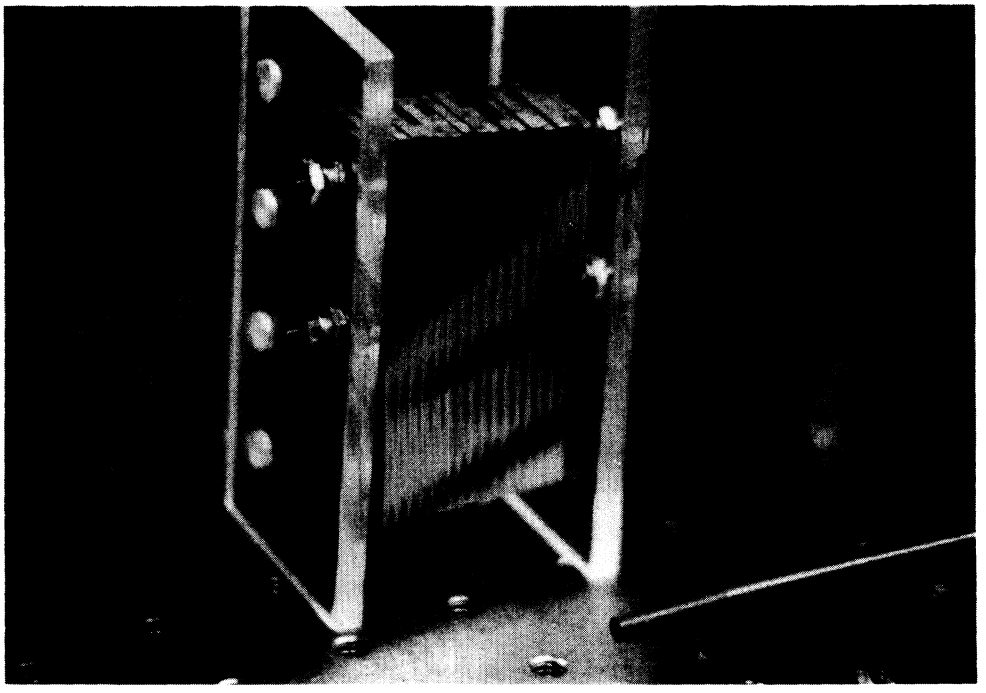

Figure 6: Photograph of constructed mirror array.

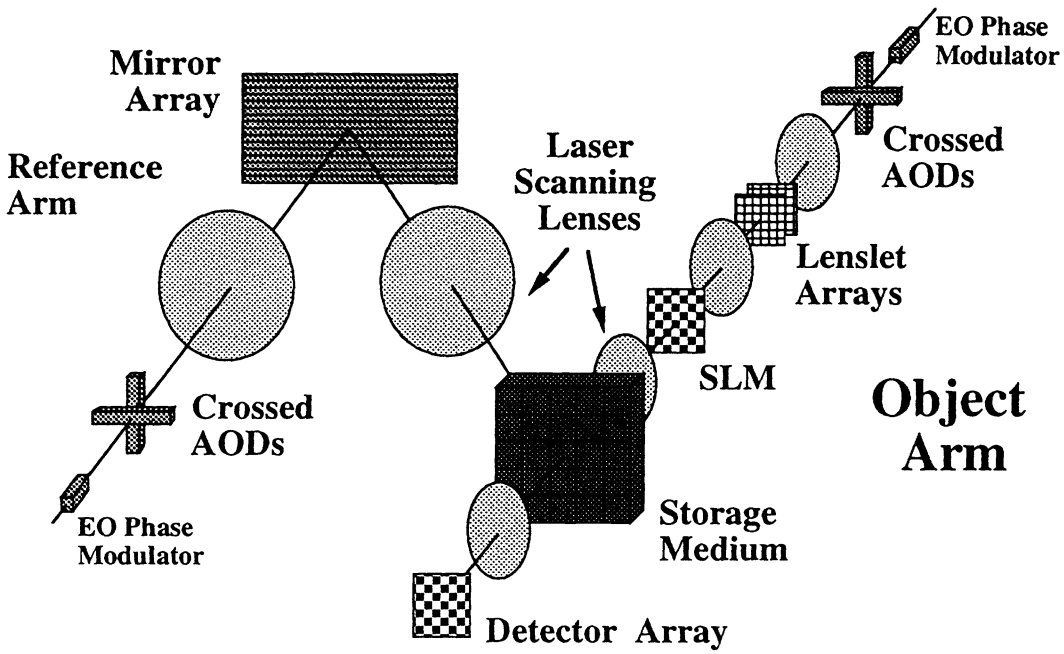

Figure 7: Holographic Random Access Memory using segmented mirror array.

FRACTAL MULTIPLEXING

We mentioned in the introduction that the reference beam angles used for separate holograms must be distinct. This distinction is easiest to create in the plane of interaction of the reference and object beams due to Bragg selectivity. Angle changes orthogonal to this plane of interaction have little effect on the phase buildup of the reconstructed hologram.

In Figure 8, we show three input reference beams (represented as vectors). Reference beams 1 and 2 define the horizontal plane of interaction, while 1 and 3 lie in the plane orthogonal to this. Reconstructions of holograms stored with beams 1 and 2 are directed along the optical axis of the original object beam, but can be recalled independently through Bragg–matching. Beam 3 reconstructs the hologram originally stored with beam 1, but the reconstruction is tilted vertically by the same angle that separates beams 1 and 3. If this tilt is larger than the vertical angular bandwidth of the image, the reconstruction of hologram #1 by beam 3 is completely displaced off the output detector. At this point, beam 3 can be used to store and independently recall a third hologram whose reconstruction falls on the original detector. This out-of-plane multiplexing was originally conceived in terms of finding non–degenerate 2–D to 2–D interconnection schemes, and the fractal name arose from the scale invariance which these patterns share.[15,16] Later, fractal multiplexing was used to store 5000 holograms at a single location.[17]

Figure 9 shows how this works in the context of the mirror array. Mirror strips 1 and 2 perform the expected spatial multiplexing at locations A and B. Mirror strip 3 is oriented parallel to strip 2, but displaced vertically. Beams deflected to strip 3 arrive at location A, but with a different vertical incidence angle than those arriving via strip 2. If the vertical separation between strips 2 and 3 is large enough relative to the vertical bandwidth of the images being stored, then each can be used to store and retrieve holograms.

EXPERIMENT

In this section, we describe an experiment combining the LILA architecture with fractal multiplexing and the mirror array. Figure 10 shows the experimental setup. In this setup, the mirror array delivers

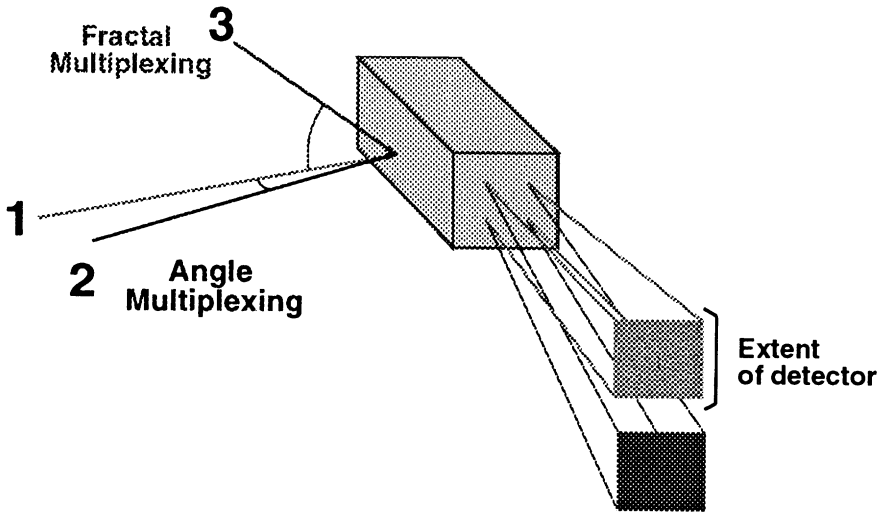

Figure 8: Fractal or out–of–plane multiplexing.

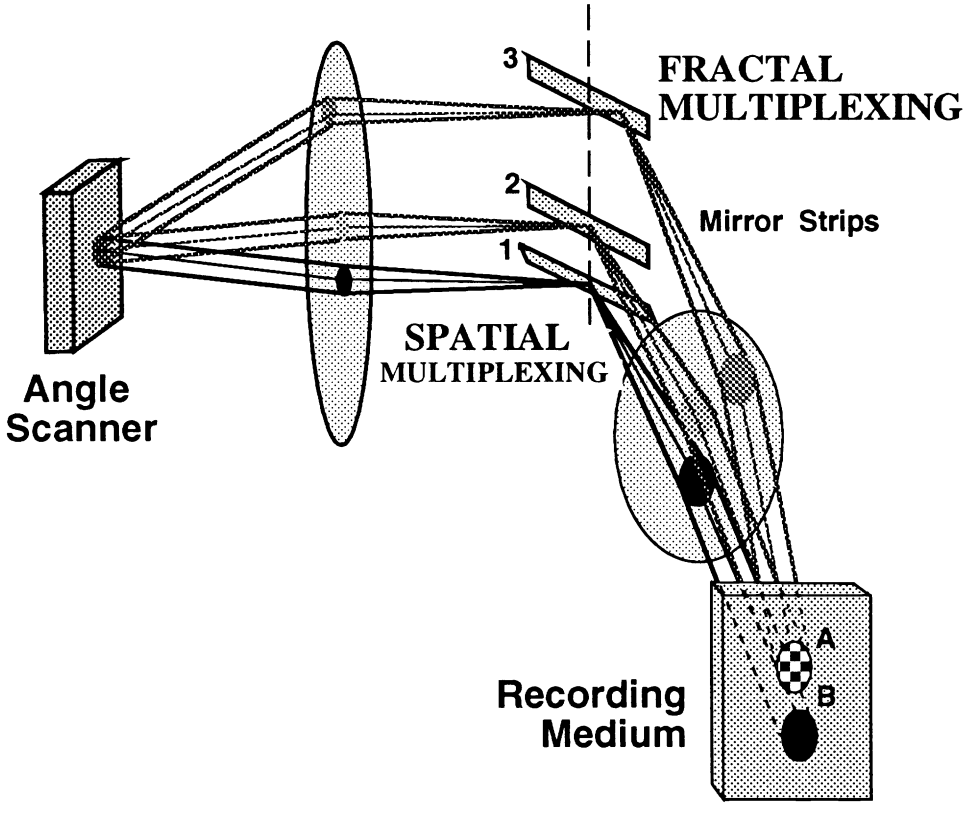

Figure 9: Implementation of fractal multiplexing with the mirror array.

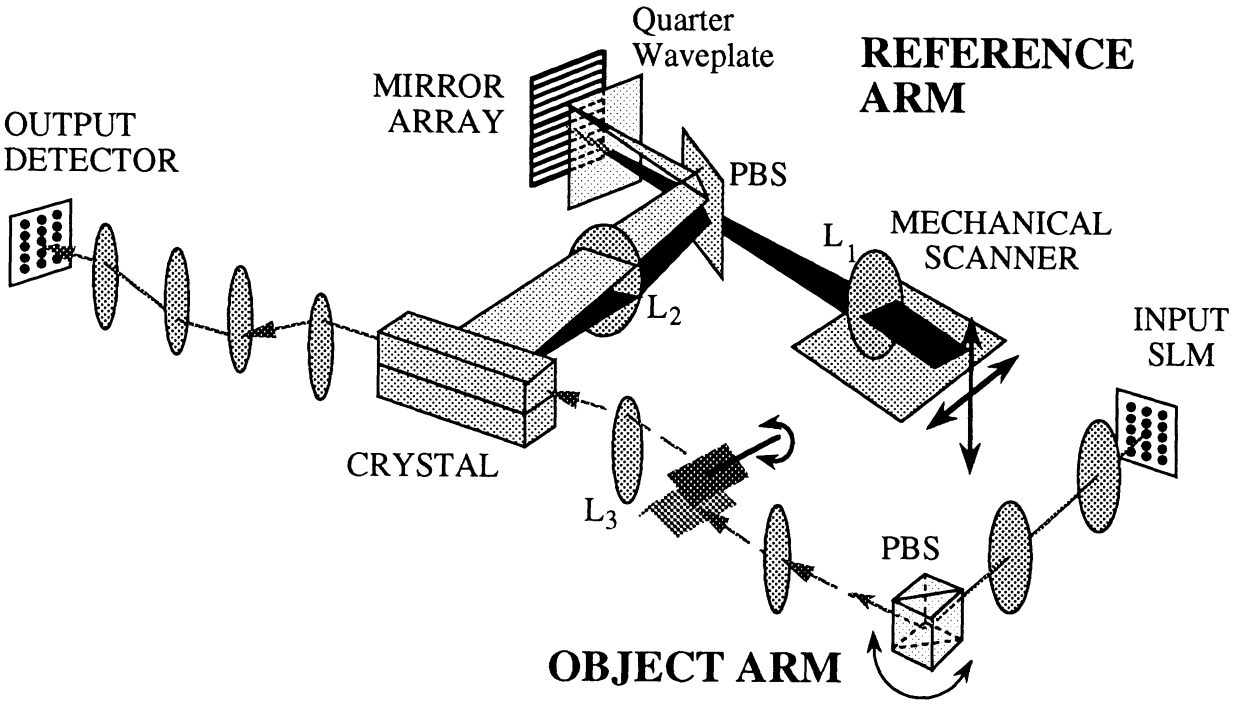

Figure 10: LILA setup with mirror array and fractal multiplexing. System is capable of storing and retrieving 160,000 holograms within the access time of a non-mechanical angle deflector.

reference beams which are wide enough to cover the side of a crystal bar. The reference arm contains an XY mechanical scanner which moves the focused reference beam across the surface of the mirror array, horizontal for angle multiplexing, vertical for fractal and spatial multiplexing. Not shown in the drawing are two cylindrical lenses which magnify the horizontal dimension of the reference beam, and two mirrors in a periscope arrangement to convey this beam onto the mechanical scanner. A 2 inch polarizing beamsplitter cube and quarter waveplate are used to increase the efficiency of the reference arm. Lenses L_1 and L_2 have focal lengths of 80 and 120mm, respectively. The reference beam spot size is elliptical, about 20mm wide and 6mm high, with an area of 0.9425 cm^2.

The object beam is directed to the proper location after the image information has already been imposed on the beam. The image presented on the SLM is demagnified by 3× and imaged to the center of a polarizing beam splitter cube mounted on a rotation stage. This horizontal deviation is not required in the theoretical design of this system, but has an important role in its practical realization. One of the difficulties of LILA storage is that as the amount of fixed pattern energy (from dust, fixed patterns on the SLM display, or common features among the presented images) increases, images become increasingly distorted. By moving the horizontal deflector several times during storage at a single vertical location, this buildup of noise gratings can be restarted and additional crystal volume used for storage.

The image plane in the center of this horizontally rotating polarizing beamsplitter cube is imaged to a pair of mirrors via a 4F system. The lower mirror is fixed and deflects the image by 90° so it falls on the upper mirror. This upper mirror is on a rotating stage (the rotation axis is horizontal), and returns the object beam to a near–horizontal path. In doing so, the vertical deflection can be set. The center of rotation of the upper mirror is in the second image plane of the object arm, so the deflection always originates from the optical axis. At this point, the object beam has deflected by an arbitrary 2–D angle. On the far side of lens L_3 (focal length 300mm), this angle determines where the Fourier transform of the displayed information arrives. Since a random phase plate is not used, the crystal is not placed in the Fourier transform plane, but is displaced beyond it by 80mm. At this point, the DC portion of the

expanding image is approximately 1.77mm high × 2.4mm wide. Three lenses after the crystal provide filtering and slight magnification, and image the reconstructed holograms onto a Photometrics Star I cooled scientific CCD. The advantage of Fourier transform storage becomes apparent at this point, since the reconstructions from all the spatially multiplexed locations can be imaged onto a single detector array.

10,000 holograms were stored in a 0.01% Fe–doped crystal bar of dimensions 10×10×20 mm. The **c**–axis was at 45° to the vertical faces. The images were displayed in text mode (80 column by 24 rows) on a 640×480 pixel VGA monitor, and sampled for the 480×440 pixel SLM. Both random bit patterns and a standard chessboard pattern were stored. The last exposure time was 0.1 second and the erasure time constant was 1200 seconds. The initial exposure lasted 0.6 seconds and the total exposure time was 35.8 minutes. The intensity of the reference beam at the crystal was 44mW/cm^2 and that of the object beam, 12.5mW/cm^2. Four mirror strips were used for storage with 2500 holograms stored on each, with an unused strip between each strip used. This was required so that the unwanted reconstructions were displaced off the detector array. The horizontal spacing between each reference beam location was 12μm, for an external angle spacing of 1×10^{-4} radians. Several reconstructions are shown in Figure 11. The average diffraction efficiency was 5×10^{-9}. The average power in the reconstructions (which were already half dark) was 2.5 times the background scatter (measured before storage).

No comprehensive study of the SNR is presented for several reasons. First, distortions in the input image were present due to the slight gaussian envelope of the collimated beam illuminating the SLM, the non–uniform polarization rotation that occurs over each SLM pixel, as well as between different pixels, and dust and other imperfections present in the elements of the object beam. Second, the image fidelity worsened when the uncoated crystal was placed in the system (before any holograms were stored). The double back–reflection off the crystal end faces appeared as a slightly shifted ghost image at the detector plan, with gain through interferometric detection with the straight–through image. Finally, all these same distortions which degraded image fidelity were also present during storage as fixed pattern noise, and were exaggerated via noise gratings during exposure of the 10,000 holograms. Since an SLM designed for modulation of coherent light combined with a AR coated crystal would not present as much fixed pattern noise during storage, the present experiment is not suitable for obtaining an accurate measure of the SNR and bit–error–rate. It is possible, however, to measure the crosstalk noise since it is not sensitive to the fidelity with which the holograms were stored. We performed a systematic study of crosstalk noise as a function of the number of holograms stored. During storage of 100, 200, 500, 1000, 2000, 5000, and 10,000 holograms, the 50^{th} location was skipped and left vacant. The light appearing at the detector when the reference beam was returned to this angle was measured, and the histogram of data values computed for the same detector area that would be occupied by the reconstructed SLM images. The star camera returns a 12–bit value for each pixel—a 1 second exposure was used for all measurements. Since this is a representation of the dark or zero level of the output hologram, the desired histogram is a very sharp peak located at very low pixel values. As can be seen in Figure 12, the crosstalk noise approaches these desired characteristics as more and more holograms are stored. By the time 10,000 holograms are stored, the crosstalk noise is very near the original background scatter measured before any holograms are stored. This trend is backed by recent theoretical crosstalk studies,[18,19] which show that crosstalk noise decays along with the signal strength as more holograms are stored. This is due to the fact that the strength of each stored hologram decays as $1/M^2$, whereas the normalized worst–case crosstalk noise grows as M.

We have also used this same Fractal/LILA/Mirror Array system shown in Figure 10 to store and reconstruct holograms at multiple locations. Three 10mm×10mm×20mm crystals were used. The system was used as was, without correcting the small error in the positioning of the rotation axes of the deflection mirrors. Two crystals were stacked together and the third was placed on a second tilt table about 3cm above the top of the lower crystal stack. Numbering locations from the bottom of the stack of LILA locations, the bottom crystal contained locations 1 and 2, the middle crystal contained locations 4 and

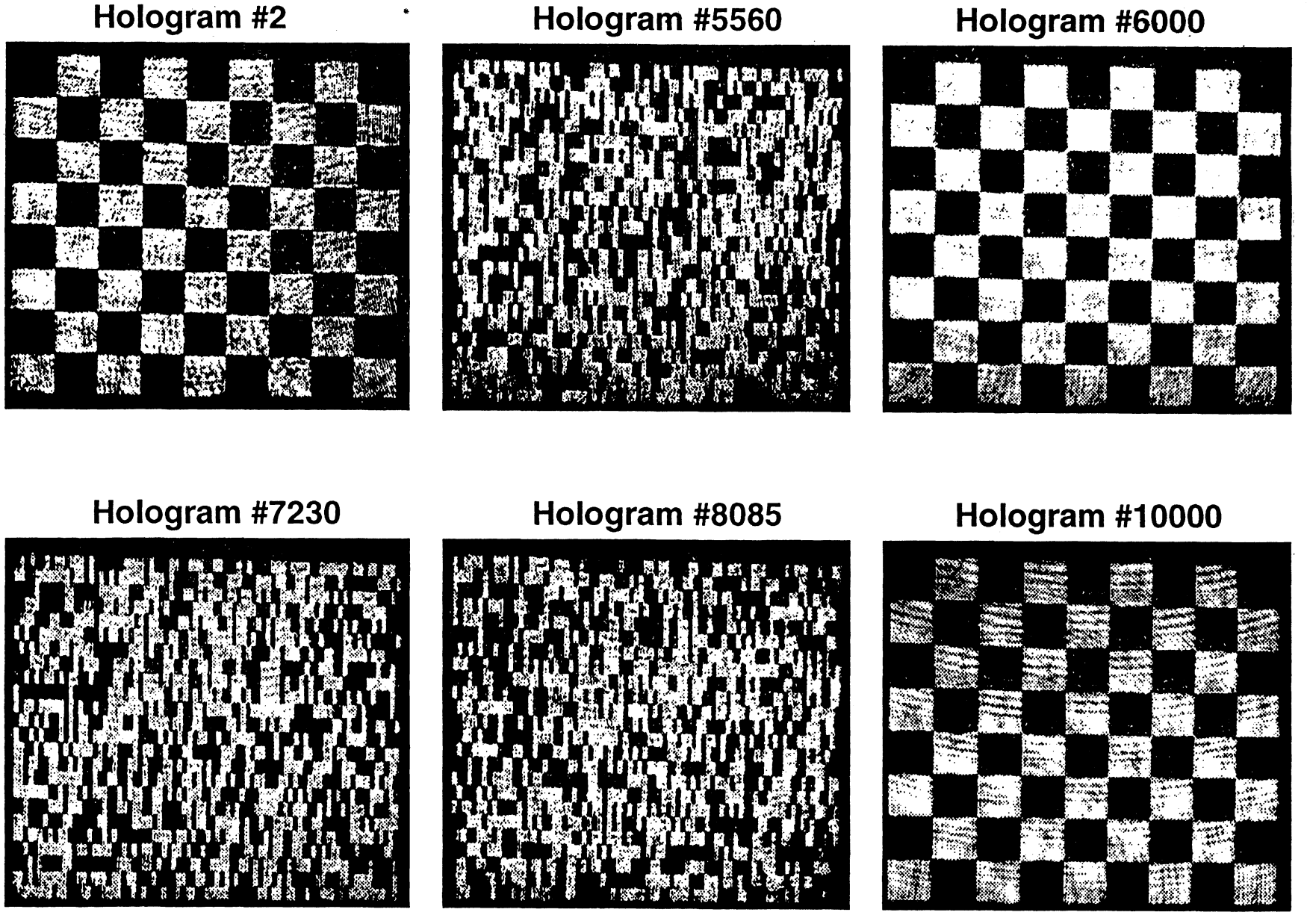

Figure 11: Reconstructions from storage of 10,000 holograms in LILA/Fractal/Mirror Array system

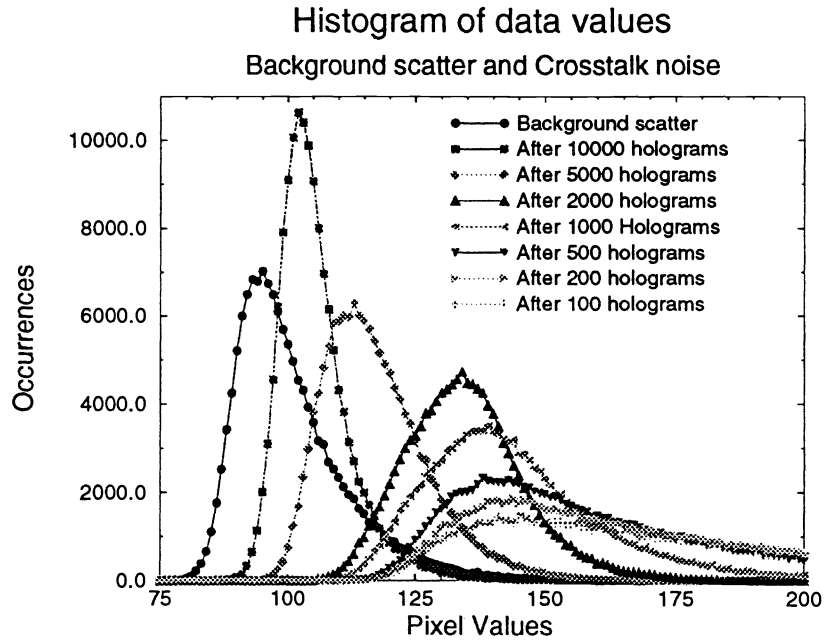

Figure 12: Histogram of data values for background scatter and crosstalk noise as a function of holograms stored

5, and the top crystal contained locations 15 and 16. Note that location 3 hit the boundary between the bottom two crystals. 100 holograms were stored at each of locations 1,2, 15, and 16, and 500 holograms at both location 4 and location 5. Some movement and slight defocusing at the output detector was noticed between the output reconstructions, but was overshadowed by the presence of the backreflection ghost images. We expect that rigorous alignment of the deflection mirrors should leave only the aberrations of the lenses and the varying wedge angles of the crystals as error sources.

CONCLUSION

We have demonstrated a system which combines the Long Interaction Length Architecture with the segmented mirror array. Fractal multiplexing is used so that several mirror strips are assigned to a each vertically separated location, dividing the SBP load on the reference beam equally between vertical and horizontal dimensions. We have demonstrated storage of 10,000 holograms at a single location, using 10% of the volume of the previous image plane experiment while maintaining diffraction efficiency and decreasing background noise. In addition, we have demonstrated simultaneous storage and recall of holograms at 6 of the 16 locations, including the lowest and highest location.

Future work includes increasing the diffraction efficiency through optimization of the interaction region and annealing of the Fe–doped $LiNbO_3$ crystals, and improving input SNR by cleaning up the input wavefronts and the optical system, as well as by AR coating the crystals used for storage. We plan to design and build second generation transmissive "mirror" arrays using diffractive optics or holographic optical elements, and incorporate non–mechanical deflectors such as AODs or liquid–crystal beam steering elements.

ACKNOWLEDGEMENTS

This work is funded by Rome Lab/IRAP under contract # 30602–94–C–0182. G. Burr acknowledges the support of an Office of Naval Research Graduate Fellowship.

REFERENCES

1. D.L. Staebler, J.J. Amodei, and W. Phillips, "Multiple storage of thick phase holograms in $LiNbO_3$," VII International Quantum Electronics Conference, Montreal, May (1972).

2. F. T. S. Yu, S. Wu, A. W. Mayers, and S. Rajan, "Wavelength multiplexed reflection matched spatial filters using $LiNbO_3$," *Optics Communications* **81,** 343 (1991).

3. G. A. Rakuljic, V. Leyva, and A. Yariv, "Optical data storage by using orthogonal wavelength–multiplexed volume holograms," *Optics Letters* **17,** 1471 (1992).

4. T. F. Krile, M. O. Hagler, W. D. Redus, and J. F. Walkup, "Multiplex holography with chirp–modulated binary phase–coded reference–beam masks," *Applied Optics* **18,** 52 (1979).

5. J. E. Ford, Y. Fainman, and S. H. Lee, "Array interconnection by phase–coded optical correlation," *Optics Letters* **15,** 1088 (1990).

6. D. Psaltis, D. Brady, and K. Wagner, "Adaptive optical networks using photorefractive crystals," *Applied Optics*, **27,** 1752 (1988).

7. G. W. Burr, F. H. Mok, and D. Psaltis, "Spatial and Angle Multiplexing using the Long Interaction Length Architecture," OSA Annual Meeting, paper TuH6, October 1993.

8. L. d'Auria, J. P. Huignard, and E. Spitz, "Holographic read–write memory and capacity enhancement by 3–D storage," *IEEE Transactions on Magnetics*, MAG–9, 83 (1973).

9. L. d'Auria, J. P. Huignard, C. Slezak, and E. Spitz, "Experimental holographic read–write memory using 3–D storage," *Applied Optics,* **13,** 808 (1974).

10. J. P. Huignard, F. Micheron, and E. Spitz, Chapter 16, *Optical Properties of Solids,* pg 847, North Holland, Amsterdam, (1976).

11. F. Mok, D. Psaltis, and G. W. Burr, "Spatially– and Angle–multiplexed Holographic Random Access Memory (invited paper)," *Proceedings of the SPIE*, **1773c**, pg 1, (1992).

12. D. Psaltis, "Parallel optical Memories," *Byte,* Sep 1992, pg 179.

13. S. Tao, D. R. Selvah, and J. E. Midwinter, "Spatioangular multiplexed storage of 750 holograms in an Fe:$LiNbO_3$ crystal," *Opt. Lett.* **18**(11), 912 (1993).

14. G. W. Burr, F. Mok, and D. Psaltis, "Large–scale Holographic Memory: Experimental Results (invited paper)," Proceedings of the SPIE, **2026–62**, (1993).

15. D. Psaltis, X.-G. Gu, and D. Brady, "Fractal sampling grids for holographic interconnections," Proceedings of the SPIE, Vol. 963, pg 468, (1988).

16. D. Psaltis, D. Brady, X. G. Gu, and S. Lin, "Holography in artificial neural networks," *Nature*, **343**, pgs 325–330, (1990).

17. F. Mok, "Angle–multiplexed storage of 5000 holograms in lithium niobate," *Opt. Lett.* **18**(11), 915 (1993).

18. C. Gu, J. Hong, I. McMichael, R. Saxena, and F. Mok, "Cross–talk–limited storage capacity of volume holographic memory," *Journal of the Optical Society of America* **A**, **9**, 11, pgs 1–6, (1992).

19. G. W. Burr, K. Curtis, and D. Psaltis, "Comparison of Wavelength– and Angle–Multiplexed Holographic Memories," OSA Topical Meeting on Optical Computing, paper OWB4, March 1993.